

Understanding the Interactions between Soft Segments in Polyurethanes: Structural Synergies in Blends of Polyester and Polycarbonate Diol Polyols

[Yuliet Paez-Amieva](#) and [José Miguel Martín-Martínez](#) *

Posted Date: 20 October 2023

doi: 10.20944/preprints202310.1335.v1

Keywords: polyester polyol; polycarbonate diol polyol; polyols blends; van der Waals interactions; Infra-red spectroscopy; differential scanning calorimetry; thermal gravimetric analysis; contact angle; X-ray photoelectron spectroscopy; plate-plate rheology; self-adhesion



Preprints.org is a free multidiscipline platform providing preprint service that is dedicated to making early versions of research outputs permanently available and citable. Preprints posted at Preprints.org appear in Web of Science, Crossref, Google Scholar, Scilit, Europe PMC.

Copyright: This is an open access article distributed under the Creative Commons Attribution License which permits unrestricted use, distribution, and reproduction in any medium, provided the original work is properly cited.

Article

Understanding the Interactions between Soft Segments in Polyurethanes: Structural Synergies in Blends of Polyester and Polycarbonate Diol Polyols

Yuliet Paez-Amieva and José Miguel Martín-Martínez *

Adhesion and Adhesives Laboratory. University of Alicante, 03080 Alicante, Spain; yuliet.paez@ua.es

* Correspondence: jm.martin@ua.es; Tel.: +34-965903977

Abstract: The extent of micro-phase separation in polyurethanes (PUs) depended on the molecular weight, the chemical nature and the structure of the polyol/soft segments. Balanced properties in PUs were obtained by using blends of polyols during synthesis. No previous studies have been devoted to understand the interactions between the soft segments that affect the properties of the PUs. In this study, different blends of two polyols of different nature (polyester – PE – and polycarbonate diol – CD) and similar molecular weight were prepared and their structural, thermal, surface, viscoelastic and self-adhesion properties were assessed. PE showed larger number of structural repeating units and higher number of polar groups than CD, but the carbonate-carbonate interactions in CD were stronger than the ester-ester interactions in PE. The blending of CD and PE imparted synergic structural properties, particularly in the ones containing less than 50% PE, they were associated to the disrupt of carbonate-carbonate interactions in CD and the formation of new ester-carbonate and hydroxyl-carbonate interactions. Therefore, higher glass transition temperatures, a new diffraction peak at $2\theta = 24^\circ$, one additional thermal degradation at 426–436 °C, and less steeper decline of the storage moduli to lower temperature were found in CD+PE blends with less than 50 wt.% PE. Furthermore, the different interactions between the polyol chains in the blends were also evidenced on their surface properties, and all CD+PE blends showed self-adhesion property which seemed related to the existence of ester-carbonate and carbonate-carbonate interactions.

Keywords: polyester polyol; polycarbonate diol polyol; polyols blends; van der Waals interactions; Infra-red spectroscopy; differential scanning calorimetry; thermal gravimetric analysis; contact angle; X-ray photoelectron spectroscopy; plate-plate rheology; self-adhesion

1. Introduction

The raw materials in the synthesis of polyurethanes (PUs) are isocyanates, polyols and chain extenders [1]. The PUs can be considered as random segmented copolymers made of soft segments (SSs) and hard segments (HSs). HSs are produced by reacting the isocyanate and the chain extender, while SSs are constituted by the interactions between the polyol chains [2]. Due to thermodynamic incompatibility between HSs and SSs, a micro-phase separation is produced in the PUs which causes a discrete micro (or nano) domain structure [3–8]. The extent of micro-phase separation in the PUs depends on several parameters such as the molecular weight, the chemical nature and the structure of the reactants, among others [9,10].

The properties of the PUs with HSs content lower than 30% are mainly determined by the interactions between SSs, i.e., between the polyol chains. The most common polyols in the synthesis of PUs are polyesters, polyethers, and, less commonly, polycaprolactones and polycarbonate diol polyols, and their molecular weights range typically between 500 and 10,000 Da. The chemical nature, structure, and molecular weight of the polyols have an important influence on the properties and performance of the PUs [11,12].

The most common polyols for synthesizing PUs are polyesters and polyethers. The polyether polyols are obtained by condensation of two alcohols with elimination of water [1] and their properties are determined primarily by the ether linkage. The PUs made with polyether polyols show

a high resistance to hydrolytic degradation, high resiliency, water vapour permeability, abrasion resistance, and flexibility at low temperatures [11], but their mechanical properties are poor [13].

The polyester polyols are obtained by polycondensation of esters obtained by reacting a carboxylic acid and an alcohol [1]. The linear polyester polyols are thermally stable below 100 °C and they react easily and quantitatively with isocyanates. The hydrolysis stability of the ester linkage is clearly inferior to that of the ether linkage because the released acid group from the ester linkage exerts an auto-catalytic effect which is deleterious to SSs of PUs. The increased hydrophobicity and the higher number of ester groups improve the resistance to hydrolytic degradation of the polyester polyols [11]. The aliphatic polyester polyols exhibit excellent tensile properties, chemical resistance, cut resistance, tear strength, and high temperature stability.

In order to improve the hydrolytic stability of the PUs, they can be synthesized with polycaprolactone or polycarbonate diol polyols. Their superior hydrolytic resistance is due to their low moisture absorption and, in the case of the polycarbonate diol polyols, the generation of CO₂ upon hydrolysis without producing acidic moieties. The PUs made with polycaprolactone polyols show high chemical resistance, good properties in a wide range of low and high temperatures, impact resistance, cut and tear resistance, sliding and abrasion resistance, and excellent durability [12]. However, the PUs made with polycarbonate diol polyols show the greatest hydrolytic resistance, and also a balanced combination of high resistance to heat, weathering, and abrasion [14].

Structurally, the polycarbonate and co-polycarbonate diols are linear, aliphatic polyols with carbonate linkages, the carbonate linkage provides high stability. There are two main synthesis procedures of the polycarbonate diol polyols: (i) Reaction of a diol with either dimethyl carbonate or diphenyl carbonate in the presence of a catalyst (tetrabutoxy titanium, dibutyltin oxide), followed by removal of the excess of reactants and mono-alcohol (methanol or phenol) under reduced pressure [15]; (ii) Reaction of CO₂ with an epoxide [16]. The polycarbonate diol polyols are primary diols and exhibit good reactivity with isocyanates. Because of the high polarity and strong carbonate bond, the PUs prepared with polycarbonate diol polyols show good mechanical properties and important degree of micro-phase separation [13,17,18]. Kojio et al. [19] established that the mechanical properties of elastomeric PUs made with polycarbonate diols were determined by the restriction of the crystallization of the soft segments. On the other hand, the PUs made with polycarbonate diol polyols show high crystallinity which affects the interactions among the polymer chains [20,21].

García-Pacios et al. [21] have synthesized waterborne polyurethane dispersions (PUDs) intended for coatings made with polyols of similar molecular weights but different natures (polyether, polyester, polycarbonate diol). The PUD obtained with polyether or polyester polyol showed a high degree of phase separation between SSs and HSs, and the best performance was obtained with the PUD coating made with polycarbonate diol, this was attributed to the higher polarity of the carbonate groups which favored the formation of additional physical bonds between SSs with respect to those obtained with polyether or polyester polyol.

Jofre-Reche et al. [2] studied the influence of the carbonate-carbonate interactions on the structure and properties of PUDs. The PUDs were synthesized with different polycarbonate diols randomly copolymerized with hexamethylene and pentamethylene (C6-C5), tetramethylene (C6-C4) and trimethylene (C6-C3). The copolymers showed two glass transition temperatures, the one at higher temperature was ascribed to the interactions between carbonate groups. It was concluded that the properties of the PUs made with polycarbonate diol copolymers were affected by the degree of phase separation between HSs and SSs, the interactions between the carbonate groups, and the existence of even or odd methylene units in the copolymer backbone.

None single polyol imparts all desired properties to the PUs, so the use of blends of polyols of different nature in their synthesis may provide balanced properties. Some previous studies [13,22–26] have shown the beneficial properties of waterborne polyurethanes (PUDs) synthesized with blends of polyols of different nature. Thus, Gündüz and Kisakürek [22] have shown that the partial replacement of polyester by polyether triol during the synthesis of PUDs imparted high hardness, superior impact resistance and flexibility. Kwak et al. [23] compared the properties of PUDs made with blends of polyester and polyether polyols, the PUD made with the blends showed intermediate

storage moduli with respect to the ones made with single polyols, but the glass transition temperature (T_g) values were similar to the one made with polyester, this was ascribed to greater crystallization ability and stronger intermolecular forces. Meng et al. [24] have synthesized PUDs with blends of ethylene oxide-propylene oxide copolymer and poly(tetramethylene ether glycol), and they exhibited excellent waterproof properties. Cakic et al. [25] have prepared PUDs with blends of polycaprolactone and polyethylene glycol or polypropylene glycol, they found a significant different influence on the degree of micro-phase separation and the extent of crystallization. In a later study [26], they studied the properties of PUDs made with blends of polypropylene glycol and polycarbonate diol, they showed improved thermal stability. On the other hand, Fuensanta et al. [13] have synthesized PUDs with blends of polyester and polycarbonate diol polyols, they found different degree of phase separation when the content of polycarbonate diol polyol was lower or greater than 50 wt.%; furthermore, complex interactions between the two types of SSs were noticed. On the other hand, upon ageing, the PUDs made with blends containing more than 50 wt.% polycarbonate diol polyol showed excellent adhesion due to the interactions between the carbonate groups in SSs and the higher miscibility between the hard and soft domains.

The previous studies have shown that the blending of polyols of different nature imparted improved mechanical, thermal, surface and adhesion properties to the PUs [10,13,21,27]. These improved properties have been ascribed to changes in the degree of micro-phase separation between HSs and SSs. Because the properties of the PUs are severely determined by the interactions between SSs, the interactions between the polyol chains of different nature would be the ultimate responsible of their different degree of phase separation. However, to the best of our knowledge, no previous studies on the interactions between polyols of different nature have been carried. The assessment of those interactions will help to understand the structural features of the PUs made with blends of polyols. Therefore, in this study, different blends of polyester and polycarbonate diol polyols of similar molecular weights were prepared and their structural, thermal, surface, viscoelastic and self-adhesion properties were assessed.

2. Materials and Methods

2.1. Materials

The raw materials were polycarbonate of 1,6 hexanediol polyol with molecular weight of 1000 Da - CD -(Eternacoll® UH-100, UBE Chemical Europe S.A., Castellón, Spain) and polyester polyol derived from 1,6 hexanediol with molecular weight of 1000 Da – PE - (Hoopol® F-523, Synthesia Española, Barcelona, Spain).

2.2. Methods

2.2.1. Preparation of the Polyols Blends

The polyols were dried under vacuum at 80 °C for 2 hours. The necessary amount of each polyol to prepare 5 g blend was added to a 15 mL polypropylene bottle maintained at 80 °C. The blend was stirred at 80 °C in double centrifuge SpeedMixer DAC 150.1 FVZ-K equipment (FlackTek Inc., Landrum, SC, USA) at 2400 rpm for 1 min. Afterward, the blends of polyols were cold down to room temperature.

The nomenclature of the polyol blends was “xCDyPE” (x and y are the percentages by weight of each polyol). Thus 2CD8PE corresponds to the blend made with 20 wt.% polycarbonate diol polyol and 80 wt.% polyester polyol.

2.2.2. Experimental Techniques

Infrared spectroscopy in attenuated total reflectance mode (ATR-IR spectroscopy). The chemical composition and the structure of the single polyols and their blends were assessed by ATR-IR spectroscopy. ATR-IR spectra were obtained in an Alpha spectrometer (Bruker Optik GmbH, Ettlinger, Germany) using a germanium prism. 60 scans were performed with a resolution of 4 cm⁻¹.

Differential Scanning Calorimetry (DSC). The structure and thermal properties of the single polyols and their blends were assessed by DSC under nitrogen atmosphere (flow rate: 100 mL/min). Two consecutive thermal runs were performed in a DSC Q100 equipment (TA Instruments, New Castle, DE, USA): (i) Heating from -80 °C to 200 °C (heating rate = 10 °C/min); and (ii) Cooling from 200 °C to -80 °C (cooling rate = 10 °C/min).

X-ray diffraction (XRD). The crystallinity of the single polyols and their blends was assessed by wide angle X-ray diffraction in a Bruker D8-Advance equipment (Bruker, Etlinger, Germany) provided with a nickel filter and a Göebel mirror. A Kritalloflex K 760-80F X-ray generator (power: 3000 W; voltage: 20-60 kV; current: 5-80 mA) and the wavelength of copper ($\lambda = 1.5406 \text{ \AA}$) were used. A scan of 2θ angles from 5° to 90° was performed by varying 0.05° every 3 seconds.

Thermal gravimetric analysis (TGA). The structure and thermal properties of the single polyols and their blends were also assessed by TGA in a TGA Q500 equipment (TA Instruments, New Castle, DE, USA) under nitrogen atmosphere (flow rate: 50 mL/min). 9–10 mg sample was placed in a platinum crucible and heated from 35 °C to 600 °C by using a heating rate of 10 °C/min. For removing char, at 600 °C, the nitrogen atmosphere was changed to air and heated for 15 min.

X-ray photoelectron spectroscopy (XPS). The chemical composition and the chemical species on the surfaces of the single polyols and their blends were assessed by XPS in a K-ALPHA instrument (Thermo Fisher Scientific, Waltham, MA, USA). The following experimental conditions were used: Aluminum $K\alpha$ radiation (1486.6 eV), twin crystal monochromator, current of 3 mA and voltage of 12 kV. A spot of 400 μm diameter was analyzed, and a hemispherical analyzer operating in the constant energy mode was used. Charge compensation was achieved with the system flood gun that provides low energy electrons and low energy argon ions from a single source. Survey scan with pass energies of 200 eV were obtained and high resolution C1s and O1s XPS spectra were obtained by using pass energies of 50 eV.

Ethylene glycol contact angle measurements. The contact angle measurements on the surfaces of the single polyols and their blends were carried out at 21 °C in an ILMS goniometer (GBX Instruments, Bourg de Péage, France) by using ethylene glycol as test liquid (purity > 99.0%, Merck-Schuchardt, Hohenbrunn, Germany). Ethylene glycol droplets of 3 μL were placed in different locations on the sample surface and measured 15 seconds after ethylene glycol drop deposition. The contact angles were the average of at least 3 drops placed on different zones of the surface with an error less than $\pm 2^\circ$.

Plate-plate rheology. The viscoelastic properties of the single polyols and their blends were assessed by plate-plate rheology in a DHR-2 rheometer (TA Instruments, New Castle, DE, USA). The samples were placed and melted at 80 °C on the lower stainless steel plate and an upper stainless steel upper plate of 20 mm diameter was used. The gap was set to 0.40 mm and a frequency of 1 Hz was used. Temperature sweep tests were carried out by cooling down from 80 °C to -20 °C by using a cooling rate of 5 °C/min.

Self-adhesion test. Cylindrical samples of the single polyols and their blends of 23.5 mm diameter and 5.6 mm high were prepared. The sample was cut by the middle with a doctor blade (Figure 1). Subsequently, the cut parts were smoothly pressed with the fingers for 30 seconds at room temperature and left to rest for 24 hours. Then, the joined samples were left falling down several times from a high of 50 cm observing if they de-bond or not. The procedure is shown in Video S1 (Supplemental Materials file) for CD.

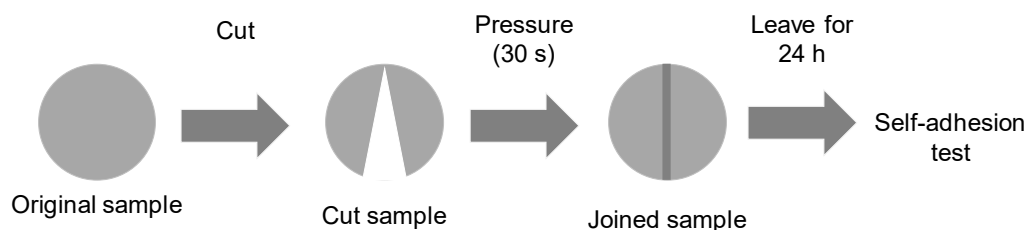


Figure 1. Assessment of the self-adhesion test of the polyols and CD+PE blends.

3. Results and Discussion

The properties of PUs with HSs content lower than 30% are mainly determined by physical interactions between SSs and the degree of micro-phase separation. The interactions among SSs depend mainly on the nature, molecular weight and structure of the polyol.

The polyester polyols imparted good mechanical properties to the PUs, but poor resistance to hydrolytic degradation [12,21]. In order to balance the hydrolytic degradation and the mechanical properties of the PUs, different blends of polyols of the same nature with different molecular weights [2,20,28] or polyols of different nature [13,21–26] have been used. The improved properties of PUs made with blends of polyols have been demonstrated, but poor attention has been paid to the interactions between SSs. It is our hypothesis that the interactions between SSs (i.e., the interactions among polyols of different nature) are the primary mechanism by which balanced and/or synergic properties are imparted to PUs. Therefore, in this study, the structural properties of different blends of polyester (PE) and polycarbonate diol (CD) polyols with similar molecular weights (1000 Da) are assessed. The structural features of the single polyols and their blends were assessed by IR spectroscopy, DSC, wide angle X-ray diffraction, TGA, XPS, contact angle measurements, and plate-plate rheology.

The structures of CD and PE (single polyols) are shown in Figures 2 and 3 respectively. Considering that the molecular weight of both polyols is 1000 Da, there are six repeating carbonate of 1,6 hexanediol units in CD and seven repeating ester of 1,6 hexanediol units in PE, i.e., PE has a larger number of structural repeating units than CD. In addition, there are 13 carbonate groups in CD and 18 ester groups in PE, and, therefore, a higher number of dipole-dipole interactions between polar groups are produced in PE than in CD. However, the carbonate-carbonate interactions in CD are stronger than the ester-ester interactions in PE. On the other hand, both CD and PE show two end primary hydroxyl groups able to interact by hydrogen bond between themselves, and with the carbonate or ester groups in the polyols. Furthermore, stronger hydroxyl-carbonate hydrogen bonds in CD than hydroxyl-ester hydrogen bonds in PE can be anticipated.

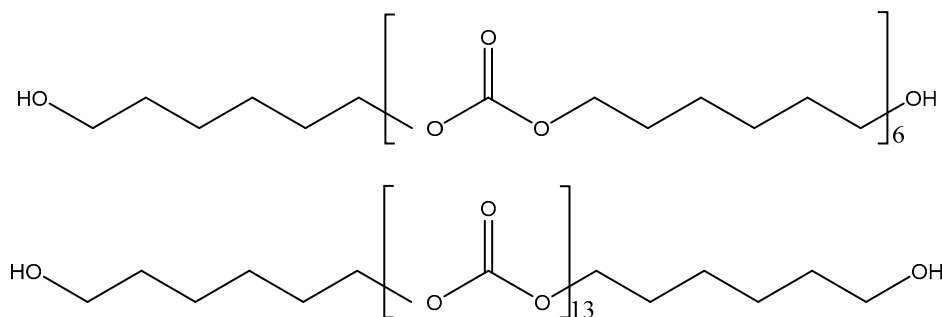


Figure 2. Chemical structure of CD (polycarbonate diol polyol).

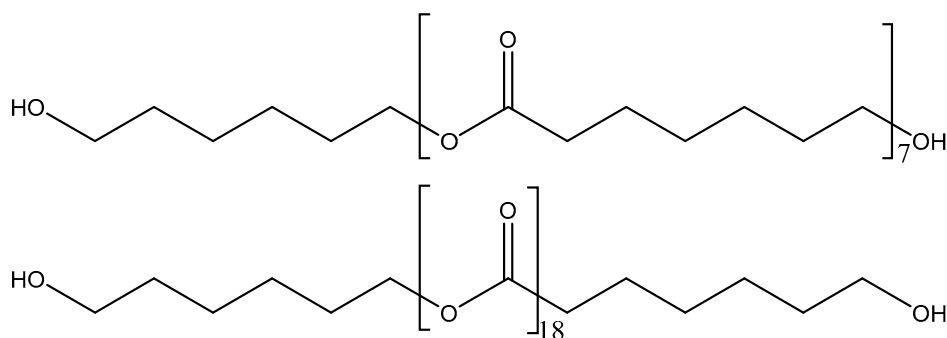


Figure 3. Chemical structure of PE (polyester polyol).

In CD+PE blends, ester-ester, carbonate-carbonate, ester-carbonate, hydroxyl-ester and hydroxyl-carbonate interactions (Figure 4) can be produced, their number and strength will differ

depending on the percentage of each polyol in the blend, and they may be different than the ones in the parent polyols.

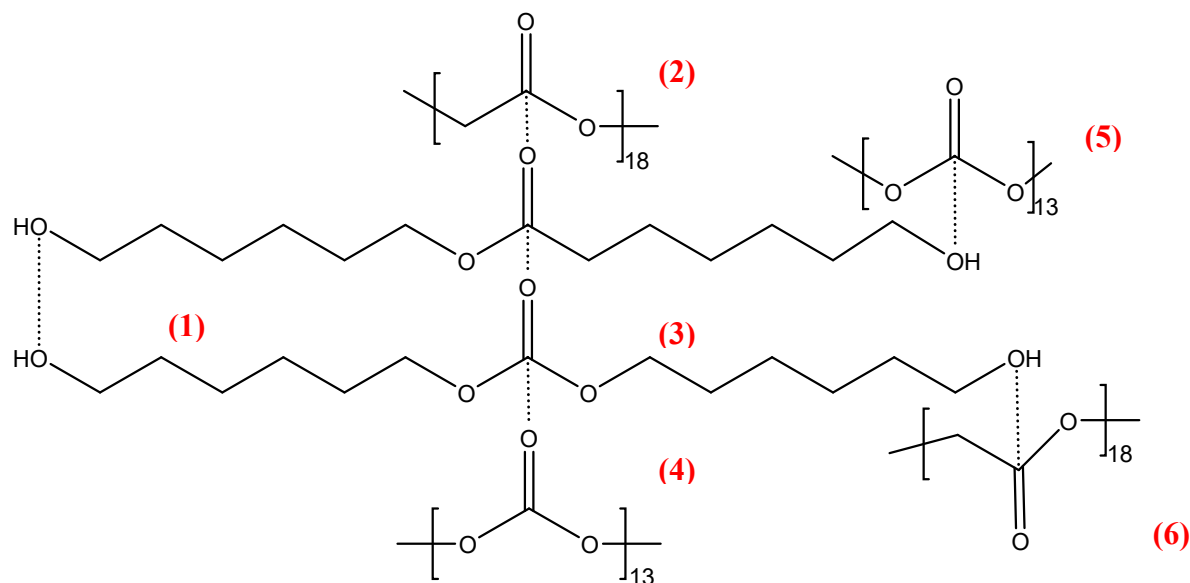


Figure 4. Potential interactions between polar groups in CD+PE blends: (1) Hydroxyl-hydroxyl; (2) ester-ester; (3) ester-carbonate; (4) carbonate-carbonate; (5) Hydroxyl-carbonate; and (6) hydroxyl-ester.

The chemical structure of the single polyols and their blends was assessed by ATR-IR spectroscopy. Figure 5 shows the ATR-IR spectra of CD, PE and CD+PE blends, and the assignment of their most characteristic IR bands are given in Tables S1–S3 of the Supplementary Materials file, respectively. All ATR-IR spectra show the same absorption bands, the main difference relies on the wavenumber of the OCC bands (1246-1257 for carbonate and ester groups, and 1171 cm^{-1} for ester group). The most intense IR bands correspond to C=O stretching at 1729-1735 cm^{-1} , OC(O)O stretching at 1246-1257 cm^{-1} and OCC stretching at 1171 cm^{-1} . The C=O stretching band appears at 1735 cm^{-1} in the ATR-IR spectrum of CD and displaces to lower wavenumber in 2CD8PE and 4CD6PE; for CD+PE blends containing more than 50% PE, the C=O stretching band appears at 1730 cm^{-1} , the same wavenumber than in the ATR-IR spectrum of PE (Table S4 of the Supplementary Materials file). On the other hand, the OC(O)O stretching band of the carbonate group appears at 1250 cm^{-1} in the ATR-IR spectrum of CD and displaces to higher wavenumber in the spectra of all blends. Therefore, different interactions between carbonyl groups are produced in CD+PE blends with respect to the parent polyols.

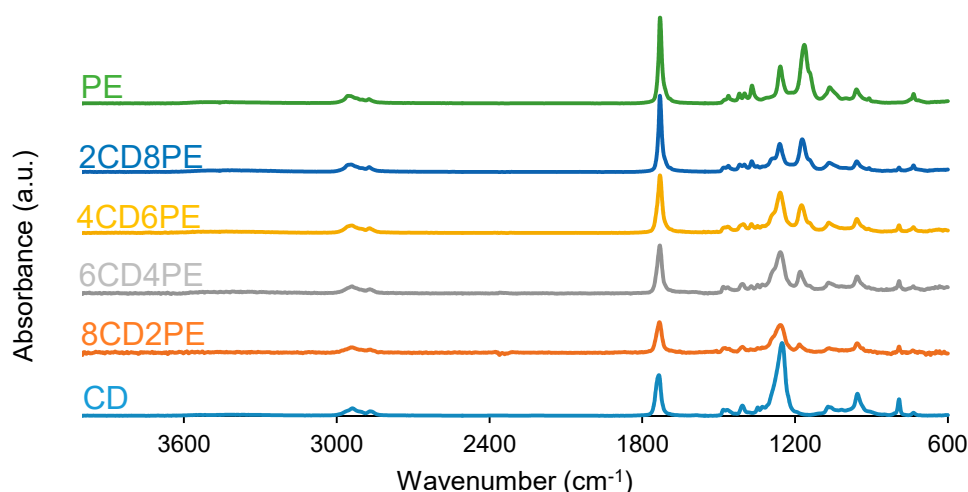


Figure 5. ATR-IR spectra of the polyols and CD+PE blends.

The number of ester groups in PE is higher than the one of carbonate groups in CD – Figures 2 and 3. Because the ratio of the intensities of the C=O band with respect to that of the OC(O)O band - $I_{C=O}/I_{OC(O)O}$ - is lower in the ATR-IR spectrum of CD than in the one of PE (Figure 6), stronger interactions between the carbonate groups in CD with respect to the ones of the ester groups in PE are evidenced. The $I_{C=O}/I_{OC(O)O}$ ratio is higher in the ATR-IR spectra of CD+PE blends than in CD, more markedly in the blends with more than 50% PE, and the $I_{C=O}/I_{OC(O)O}$ ratio in 2CD8PE is even higher than the one in PE (Figure 6). Therefore, the interactions between the ester and carbonate groups in CD+PE blends differ with respect to the ones in PE and CD and they depend on the PE content. On the other hand, the ratio of the intensities of the OC(O)O band (common to PE and CD) with respect to that of the OCC band (only in PE) - $I_{OC(O)O}/I_{OCC}$ - in the ATR-IR spectra of CD+PE blends increases sharply when the amount of PE is higher than 50 wt.% (Figure 6). 2CD8PE and PE show almost equal $I_{OC(O)O}/I_{OCC}$ ratios because similar interactions between ester groups in both. On the other hand, the variation of the $I_{C=O}/I_{OC(O)O}$ and $I_{OC(O)O}/I_{OCC}$ ratios as a function of PE amount is not linear (Figure 6), this indicates different interactions between CD and PE chains in the different blends with respect to the parent polyols.

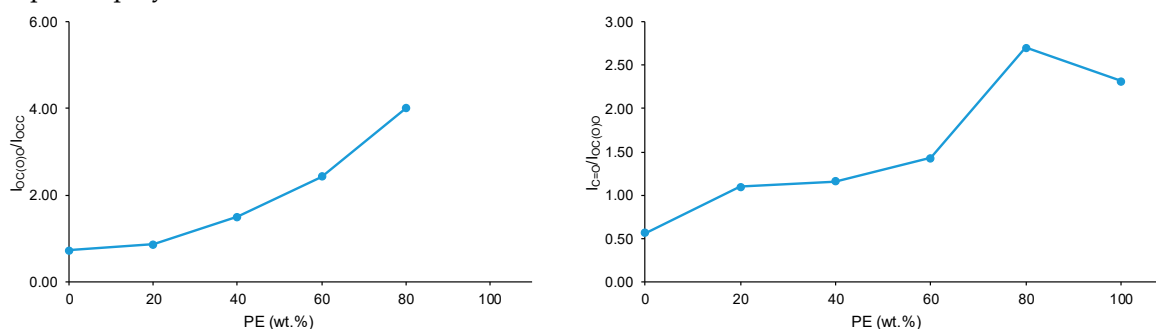


Figure 6. Variation of the $I_{OC(O)O}/I_{OCC}$ (left) and $I_{C=O}/I_{OC(O)O}$ (right) ratios of CD+PE blends as a function of PE amount.

The interactions between the polar groups in the single polyols and their blends can be better evidenced by curve fitting of the carbonyl stretching region of the ATR-IR spectra. In this study, the curve fitting of the C=O stretching band was carried out by adjusting to a Gaussian function. The curve fitting of the carbonyl region of CD (Figure 7) shows 36% free C=O of the carbonate group at 1741 cm^{-1} and 64% bonded by dipole-dipole interactions C=O groups at 1730 cm^{-1} , this confirming a

strong interaction between the carbonate groups. The assignment of these groups is in agreement with the study by Niemczyk et al. [8] whose reported three different contributions to the carbonyl region in PU made with polycarbonate diol polyol: (i) Free carbonyl groups at 1744 cm^{-1} ; (ii) carbonyl groups bonded by dipole-dipole interactions at 1731 cm^{-1} ; and (iii) hydrogen bonds between the OH group of the polyol and C=O of the carbonate at 1719 cm^{-1} . On the other hand, the curve fitting of the carbonyl region of PE (Figure 7) shows 88% free C=O of the ester group at 1730 cm^{-1} , 8% bonded by dipole-dipole interactions C=O groups at 1712 cm^{-1} , and 4% hydrogen bonded OH-ester groups at 1689 cm^{-1} . Thus, the most ester groups in PE are free and a few hydrogen bonds between the terminal hydroxyl groups and the ester groups are produced. In a previous study [29] the existence of two contributions in the C=O region in hyperbranched polyester at 1741 cm^{-1} (free carbonyl) and 1728 cm^{-1} (OH-ester hydrogen bond) have been reported.

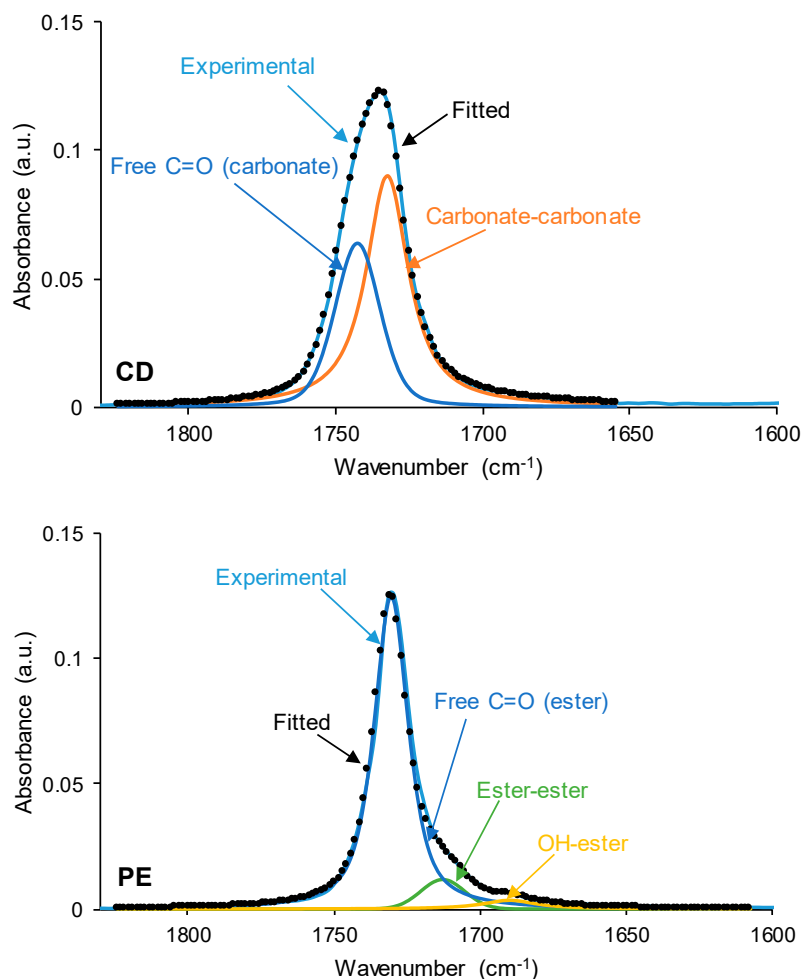


Figure 7. Curve fitting of the carbonyl stretching region of the ATR-IR spectra of CD and PE.

The curve fitting of the carbonyl stretching region of the ATR-IR spectra of the CD+PE blends are shown in Figure 8 and Figure S1 of the Supplementary Materials file. All CD+PE blends show five contributions to the carbonyl region (2CD8PE is an exception because the same three contributions than in PE are distinguished) (Table 1), the one at $1675\text{--}1689\text{ cm}^{-1}$ is ascribed to hydroxyl-carbonate interactions. The wavenumber at which each contribution appears varies depending on the amount of PE in the blend (Table S4 of the Supplementary Materials file), this evidences the existence of different interactions in CD+PE blends with respect to the parent polyols. Thus, the addition of 20% PE to CD (8CD2PE) decreases the percentages of free carbonate and carbonate-carbonate interactions, and new contributions due to carbonate-ester, hydroxyl-ester and hydroxyl-carbonate can be distinguished (Table 1), these interactions differ from the ones in CD and PE. The same contributions to the carbonyl region appear in 6CD4PE, but a lower percentage of free carbonate groups and more

important contributions of carbonate-carbonate, hydroxyl-ester and hydroxyl carbonate are obtained (Table 1); furthermore, these contributions appear at lower wavenumber (Table S4 of the Supplementary Materials file), this indicate more net interactions between the polar groups at the expense of carbonate-carbonate interactions. In 4CD6PE, the same five contributions to the carbonyl region than in 8CD2PE and 60 CD4PE can be distinguished, but the percentages of carbonate-carbonate and hydroxyl-carbonate contributions are lower and the ones of ester-ester and hydroxyl ester are higher (Table 1), and the wavenumber of the ester-ester contribution is higher (Table S4 of the Supplementary Materials file). However, the same contributions to the carbonyl stretching band are found in 2CD8PE and PE because the addition of 20% CD does not alter significantly the interactions between polar groups in PE. Therefore, the interactions between the carbonyl groups of CD and PE change in the blends, particularly in the blends containing less than 50% PE.

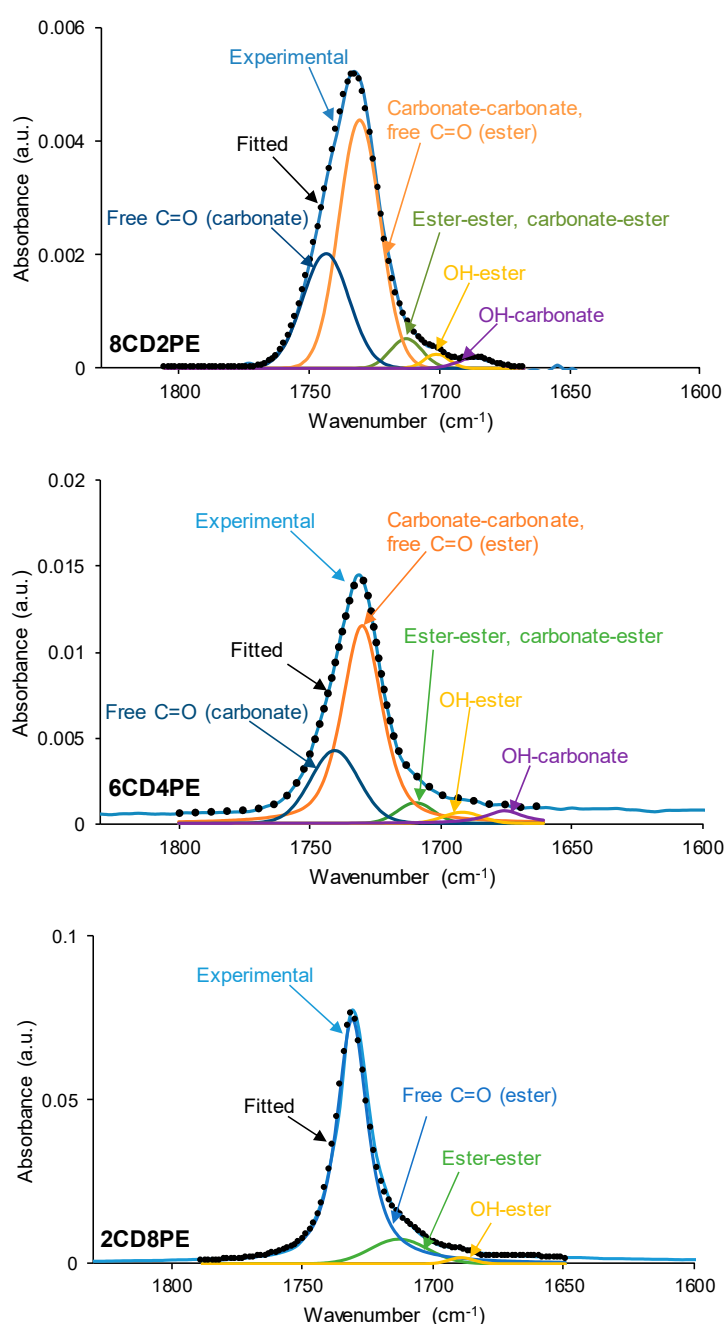


Figure 8. Curve fitting of the carbonyl stretching region of the ATR-IR spectra of some CD+PE blends.

Table 1. Percentages of C=O species in the carbonyl stretching region of the ATR-IR spectra of CD+PE blends.

Wavenumber (cm ⁻¹)	Percentage (%)				Assignment
	8CD2PE	6CD4PE	4CD6PE	2CD8PE	
1675-1689	2	4	2	-	OH-carbonate
1691-1702	2	3	3	1	OH-ester
1709-1718	5	5	14	11	Carbonate-ester, ester-ester
1729-1730	60	64	54	88	Carbonate-carbonate, Free C=O (ester)
1739-1743	31	24	27	-	Free C=O (carbonate)

The structural features of the polyols and CD+PE blends were also assessed by DSC. The DSC curves of the first heating run are given in Figure 9. All polyols and blends show two glass transition temperatures: T_{g1} (between -16 °C and -29 °C), due van der Waals interactions between polyols chains; and T_{g2} (between 1 °C and 15 °C) due to ester-ester, ester-carbonate and carbonate-carbonate interactions [2,21]. The highest T_{g1} and heat capacity at constant pressure (ΔC_{p1}) values correspond to CD and 8CD4PE due to more net interactions between the polyol chains (Table 2). The other blends show similar T_{g1} and ΔC_{p1} values because of similar interactions between the polymer chains; however, the ΔC_{p1} value in PE is lower than in the blends, this indicates the existence of stronger interactions between ester and carbonate groups in CD+PE blends. On the other hand, the highest T_{g2} and ΔC_{p2} values are found in CD and the blends with less than 50% PE (11-15 °C), and lower T_{g2} and ΔC_{p2} values are obtained by increasing the PE content (Table 2). It should be noted that the ΔC_{p1} and ΔC_{p2} values of 8CD2PE are higher than the ones in CD, this indicates the existence of ester-carbonate interactions in the blend. On the other hand, a melting at 43-48 °C is evidenced in the DSC curves of the polyols and their blends. Because the melting enthalpy is higher in PE than in CD, the melting enthalpies of the blends increase by increasing their PE content (Table 2); however, the melting enthalpy of 8CD2PE is similar to the one of PE (74 J/g), even its contains 20% PE only. Therefore, the values of the different thermal events of the first DSC heating run in CD+PE blends are different than in the parent polyols, particularly in the blends containing less than 50% PE, this confirm the existence of additional interactions (mainly ester-carbonate interactions according to IR spectroscopy studies).

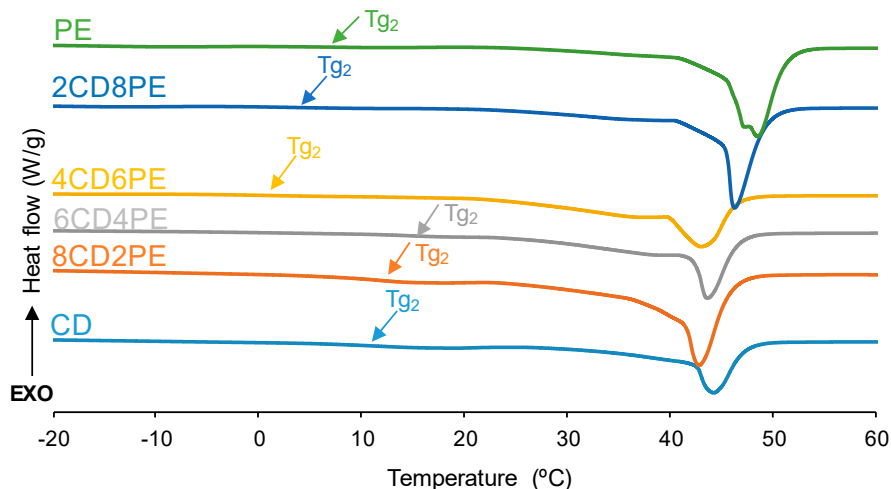
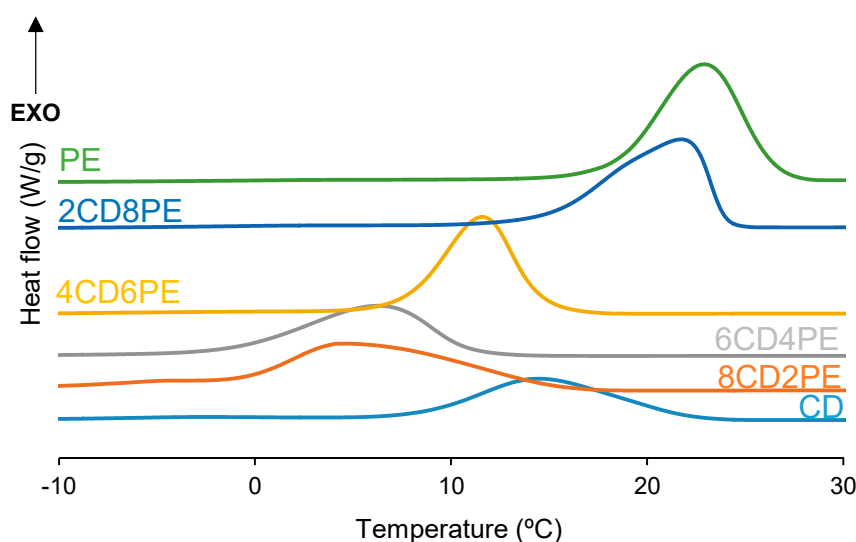
**Figure 9.** DSC curves of the polyols and CD+PE blends. First heating run.

Table 2. Thermal events in the DSC curves of the polyols and CD+PE blends. First heating run.

Polyol	T_{g1} (°C)	Δc_{p1} (J/g·°C)	T_{g2} (°C)	Δc_{p2} (J/g·°C)	T_m (°C)	ΔH_m (J/g)
CD	-16	0.34	11	0.58	44	40
8CD4PE	-16	0.43	12	0.97	43	74
6CD4PE	-27	0.18	15	0.29	43	55
4CD6PE	-27	0.19	1	0.17	43	70
2CD8PE	-29	0.21	4	0.16	46	70
PE	-28	0.14	7	0.10	48	74

After the first DSC heating run, the polyols and CD+PE blends were slowly cooled down to -80 °C and one crystallization peak at 5-23 °C with crystallization enthalpies of 45-78 J/g were found (Figure 10). PE exhibits the highest temperature and enthalpy of crystallization and CD shows the lowest ones. Therefore, an increase of the temperature and enthalpy of crystallization in the CD+PE blends can be expected. Whereas the crystallization enthalpy of the blends increases by increasing their PE content, except in 8CD2PE (Figure 11), the crystallization temperatures of the blends with less than 50% PE are lower (5-6 °C) than the one of CD (14 °C), and higher and almost similar temperatures of crystallization are obtained in 2CD8PE and PE. Therefore, the interactions between PE and CD chains in the blends differ from the parent polyol and they are stronger in the blends with less than 50% PE.

Wide-angle X-ray diffraction allows the assessment of the crystallinity of the polyols and CD+PE blends. The X-ray diffractogram of PE (Figure 12) shows two main intense diffraction peaks at 2θ values of 21° and 22°, and three additional low intense diffraction peaks at 2θ values of 17°, 23° and 29° can be distinguished. The X-ray diffractogram of CD (Figure 12) shows two main intense diffraction peaks at 2θ values of 19° and 23° (they are less intense than the ones of PE), and another low intense peak at 2θ value of 14° also appears. Therefore, CD is less crystalline than PE and the nature of the crystallinity is different in both polyols.

**Figure 10.** DSC curves of the polyols and CD+PE blends. Cooling run.

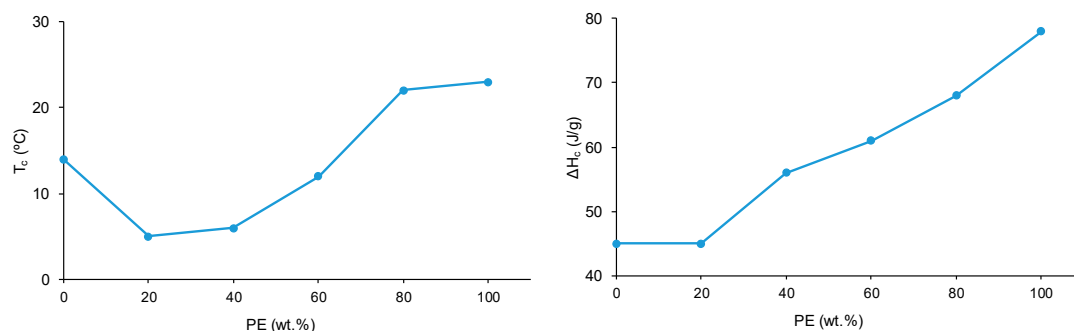


Figure 11. Variation of the crystallization temperature (left) and enthalpy (right) of CD+PE blends as a function of the amount of PE. Cooling DSC run.

The X-ray diffractograms of the CD+PE blends show different peaks with different intensities depending on their PE content. The X-ray diffractogram of 8CD2PE shows four diffraction peaks at 2θ values of 20° , 21° , 23° and 24° (Figure 12), the ones at 2θ values of 20° and 23° are the most intense. These two peaks can be ascribed to the interactions between CD chains. Because the peak at 2θ value of 20° appears at 19° in CD and its intensity is higher in 8CD2PE, stronger and different interactions (likely ester-carbonate interactions) in 8CD2PE than in CD are evidenced (Figure 13). Therefore, the addition of only 20% PE disrupts the carbonate-carbonate interactions between CD chains producing new interactions. In fact, whereas the peak at 2θ value of 21° in 8CD2PE can be ascribed to ester-ester interactions, the one at 2θ value of 24° does not appear in the parent polyols and can be ascribed to new ester-carbonate interactions. The X-ray diffractogram of 6CD4PE shows somewhat similar features than the one of 8CD2PE, but the intensity of the peak at $2\theta = 21^\circ$ (ester-ester interactions) is higher and the one at $2\theta = 23^\circ$ (carbonate-carbonate interactions) is lower (Figure 13). Furthermore, two small diffraction peaks at 2θ values of 21.3° and 22° can be distinguished, they do not appear in the parent polyols and correspond to new interactions.

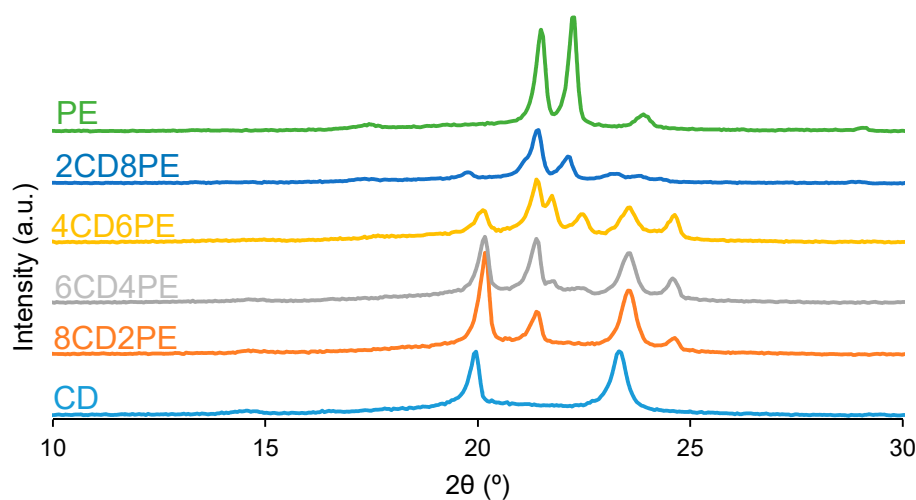


Figure 12. X-ray diffractograms of the polyols and CD+PE blends.

The X-ray diffractogram of 4CD6PE (Figure 12) shows five intense peaks at 2θ values of 20° , 21° , 22° , 23° and 24° . The peaks at 2θ values of 21° and 22° can be ascribed to ester-ester interactions and both are less intense than in PE. The peaks at 2θ values of 20° and 23° correspond to carbonate-carbonate interactions and they are much less intense than in CD. The peak at 2θ value of 24° does not exist in the parent polyols, this could be an indication of the existence of ester-carbonate interactions. The X-ray diffractograms of 2CD8PE and PE are very similar and they show two main diffraction peaks at 2θ values of 21° and 22° (Figure 12); however, the relative intensities of these two

diffraction peaks are different and additional low intense peaks at 2θ values of 20° and 23° due to CD appear in 2CD8PE.

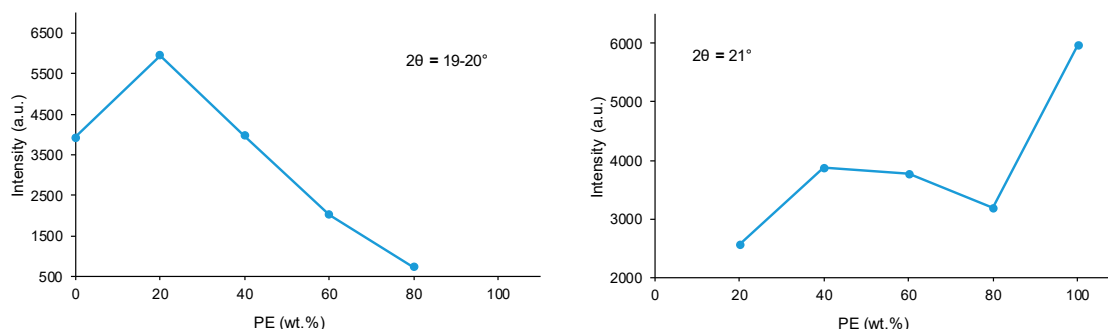


Figure 13. Variation of the intensity of the peaks at 2θ values of $19-20^\circ$ (left) and 21° (right) of the CD+PE blends as a function of the amount of PE. X-ray diffractograms.

Figure 13 shows the variation of the intensity of the diffraction peak at 2θ values of $19-20^\circ$ in CD+PE blends, this peak only appears in the X-ray diffractogram of CD and can be attributed to carbonate-carbonate interactions. The addition of 20% PE only increases the intensity of the peak and by further increasing the amount of PE in the blend, the intensity of the peak at $2\theta = 19-20^\circ$ decreases gradually. The intensity of the diffraction peak at 2θ value of 21° due to PE (ester-ester interactions) is small in 8CD2PE and increases in the blend containing 40% PE (Figure 13); the blends containing 40-80% PE show almost similar intensity of the diffraction peak at $2\theta = 21^\circ$, even their very different PE content, this indicates the existence of similar interactions (likely ester-carbonate interactions).

The structural features of the polyols and CD+PE blends were also assessed by TGA. Figure 14 shows one main thermal degradation in PE starting at 257°C and two thermal degradations in CD starting at 214°C and 301°C . The thermal degradation in CD starting at 214°C is displaced to higher temperature in the CD+PE blends, the displacement is more marked by increasing the PE content. Furthermore, the TGA curves of 8CD2PE and 6CD4PE show an additional thermal degradation starting at 350°C and 365°C , respectively, this thermal degradation is not present in the TGA curves of the parent polyols nor in the blends with PE content higher than 50%, and can be ascribed to ester-carbonate interactions. The differences in thermal stabilities can be evidenced by the temperatures at which 5% ($T_{5\%}$) and 50% ($T_{50\%}$) mass loss are produced in the TGA curves. The $T_{5\%}$ and $T_{50\%}$ values of PE are higher than in CD, and the values of the blends are intermediate, the variation of the $T_{5\%}$ and $T_{50\%}$ values as a function of the PE content is not linear (Figure 15).

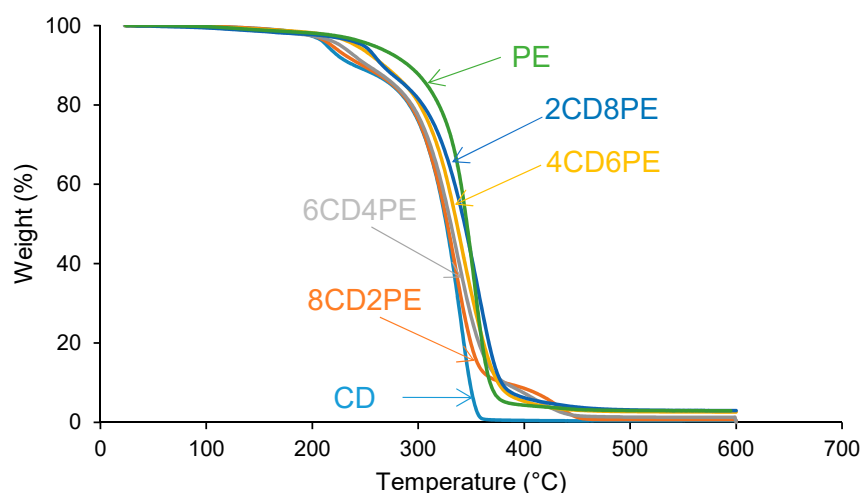


Figure 14. TGA curves of the polyols and CD+PE blends.

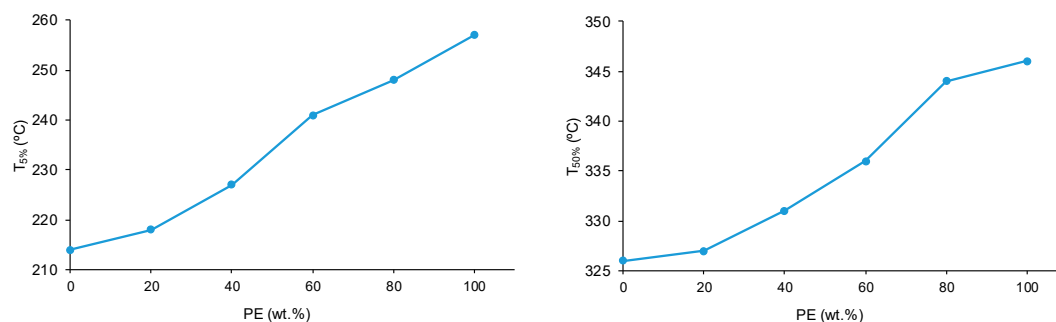


Figure 15. Variation of the temperature at which 5% (left) and 50% (right) mass loss are produced in CD+PE blends as a function of the amount of PE. TGA experiments.

The differences in the TGA curves of the polyols and CD+PE blends can be better evidenced in the derivative of the TGA curves (DTGA curves) (Figure 16). The DMTA curve of CD shows two thermal degradations at 214 °C (likely due to carbonate-carbonate interactions) and 340 °C (likely due to the interactions between the chains), the main weight loss is produced at 340 °C. The DMTA curve of PE shows one thermal degradation at 352 °C, the higher thermal stability of PE can be ascribed to the higher number of polar groups than in CD. The DMTA curves of the blends with less than 50% PE show three thermal degradations at 220-229 °C, 335-338 °C and 426-436 °C. The thermal degradations at 220-229 °C and 335-338 °C in the blends are also present in the DMTA curve of CD, but they appear at higher temperatures – the higher the PE content, the higher the degradation temperature. Furthermore, the increase of the temperature of the thermal degradation at 220-229 °C is more marked in the blends with less than 50% PE (Figure 17), whereas the one at 335-338 °C is more marked in the blends with more than 50% PE (Figure 17). Therefore, in the blends with less than 50% PE, part of the carbonate-carbonate interactions is substituted by ester-polycarbonate interactions. Furthermore, the existence of a thermal degradation at 426-436 °C in 8CD2PE and 6CD4PE blends indicates the existence of novel interactions between the polyol chains, likely ester-carbonate interactions.

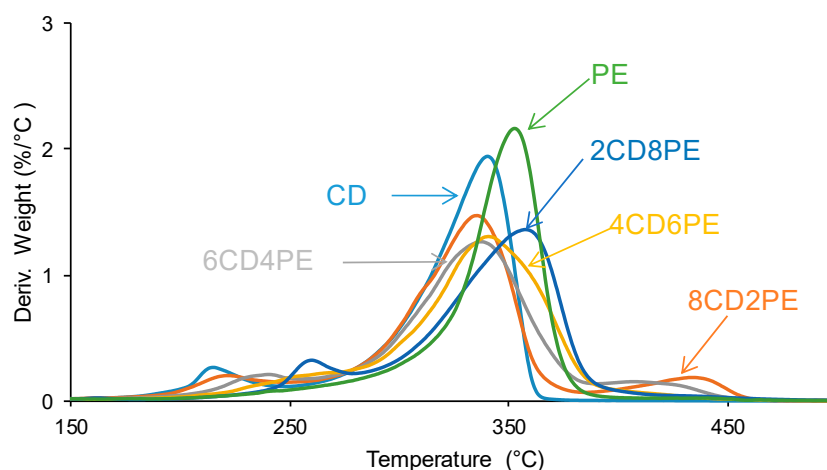


Figure 16. Derivative of the weight loss (DTGA) curves of the polyols and CD+PE blends. DTGA experiments.

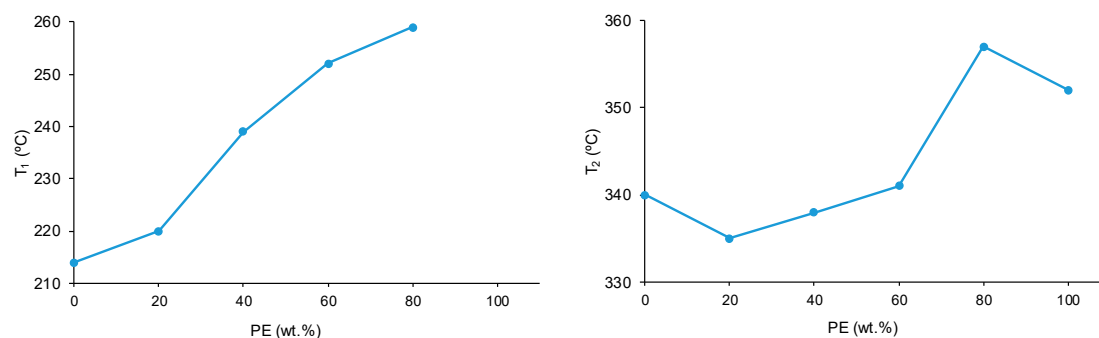


Figure 17. Variation of the degradation temperatures of CD+PE blends as a function of the amount of PE. DTGA experiments.

The structural features of the polyols and CD+PE blends may also affect their viscoelastic properties, they were assessed by plate-plate rheology. Figure 18 shows the variation of the storage modulus (G') as a function of the temperature for the polyols and their blends. In the glassy region, the storage moduli do not change by increasing the temperature. At a given temperature, all polyols and blends show a sudden decrease of the storage moduli, the temperature differs in the polyols and CD+PE blends. The temperature at which G' starts to decrease is significantly higher in PE (30 °C) than in CD (22 °C), because the higher number of ester groups in PE than carbonate groups in CD, but both show an abrupt decrease of G' in a short temperature range. The addition of 80 wt.% PE produces a decrease of G' at an intermediate temperature among the ones of PE and CD, this is an indication of the disruption of some ester-ester interactions between the PE chains in 2CD8PE. However, the addition of 20-60 wt.% PE causes a decline of G' at lower temperature than in the parent polyols and the decrease of G' with the temperature is less steeper, the higher the CD content, the more noticeable are those changes. Therefore, in the blends containing 20-60 wt.% PE, the carbonate-carbonate interactions become less important and the existence of ester-carbonate interactions are evidenced by the less steep decrease of G' with temperature. Therefore, the different interactions in CD+PE blends containing less than 40 wt.% PE cause different viscoelastic properties.

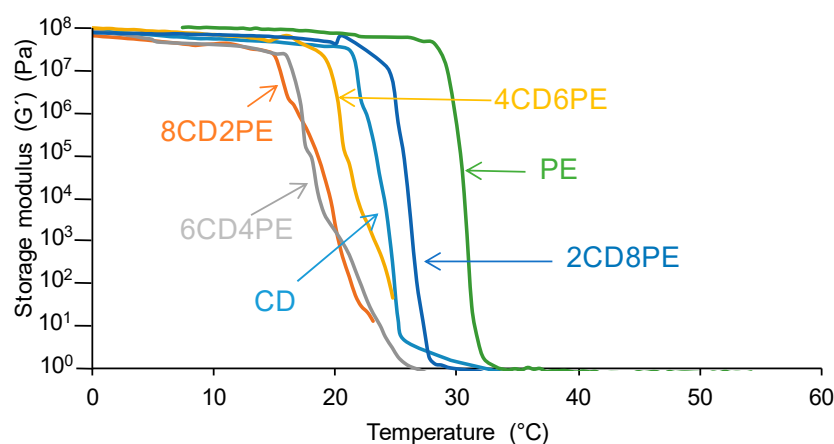


Figure 18. Variation of the storage (G') moduli of the polyols and CD+PE blends as a function of the temperature. Plate-plate rheology experiments.

All polyols and blends show a cross-over of the storage (G') and loss (G'') moduli (Figure S2 of the Supplementary Materials file). The temperature at the cross-over ($T_{\text{cross-over}}$) is related to the interactions between the polymer chains, the higher the $T_{\text{cross-over}}$ value, the higher the interactions. Figure 19 shows that PE has higher $T_{\text{cross-over}}$ value than CD because of the higher number of ester-ester than carbonate-carbonate interactions. The addition of 20 wt.% PE decreases the $T_{\text{cross-over}}$ value

of CD because the disruption of carbonate-carbonate interactions, and the addition of higher amounts of PE increases gradually the $T_{\text{cross-over}}$ value, likely due to the creation of ester-carbonate interactions.

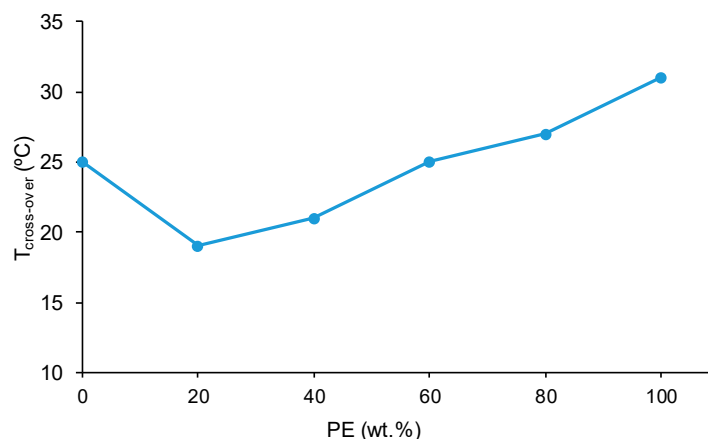
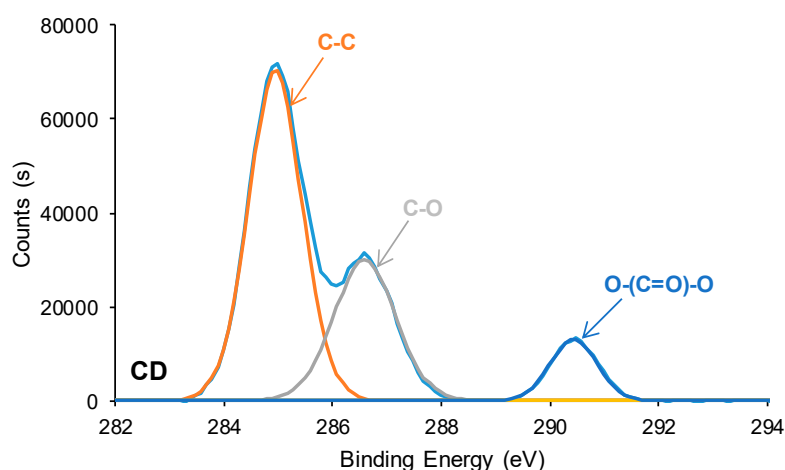


Figure 19. Variation of the temperature at the cross-over of the storage and loss moduli of CD+PE blends as a function of the amount of PE.

The different interactions between the polyol chains in the CD+PE blends may also affect their surface properties, they were assessed by XPS and contact angle measurements.

The elemental composition on the surfaces of the polyols and CD+PE blends consists on 72-74 at.% carbon and 26-28 at.% oxygen, they are similar in all polyols and blends. The chemical species on the polyols and CD+PE surfaces were assessed from the XPS high resolution C1s spectra. The C1s photopeak of CD (Figure 20) shows three different chemical species: 60 at.% C-C/C-H species at binding energy of 285.0 eV; 30 at.% C-O species at binding energy of 286.5 eV; and 10 at.% O-(C=O)-O species at binding energy of 290.5 eV (Table 3). This assignment was made according to Mishra et al. [30] XPS studies on polymers. On the other hand, the C1s photopeak of PE (Figure 20) also shows three different chemical species: 60 at.% C-C/C-H species at binding energy of 285.0 eV; 24 at.% C-O species at binding energy of 286.5 eV; and 16 at.% C=O species at binding energy of 289.0 eV (Table 3). The C1s photopeaks of CD+PE blends show four different chemical species (C-C/C-H, C-O, C=O, O-(C=O)-O), their percentages differ depending on their PE content (Figures 20 and S3 of the Supplementary Materials file).



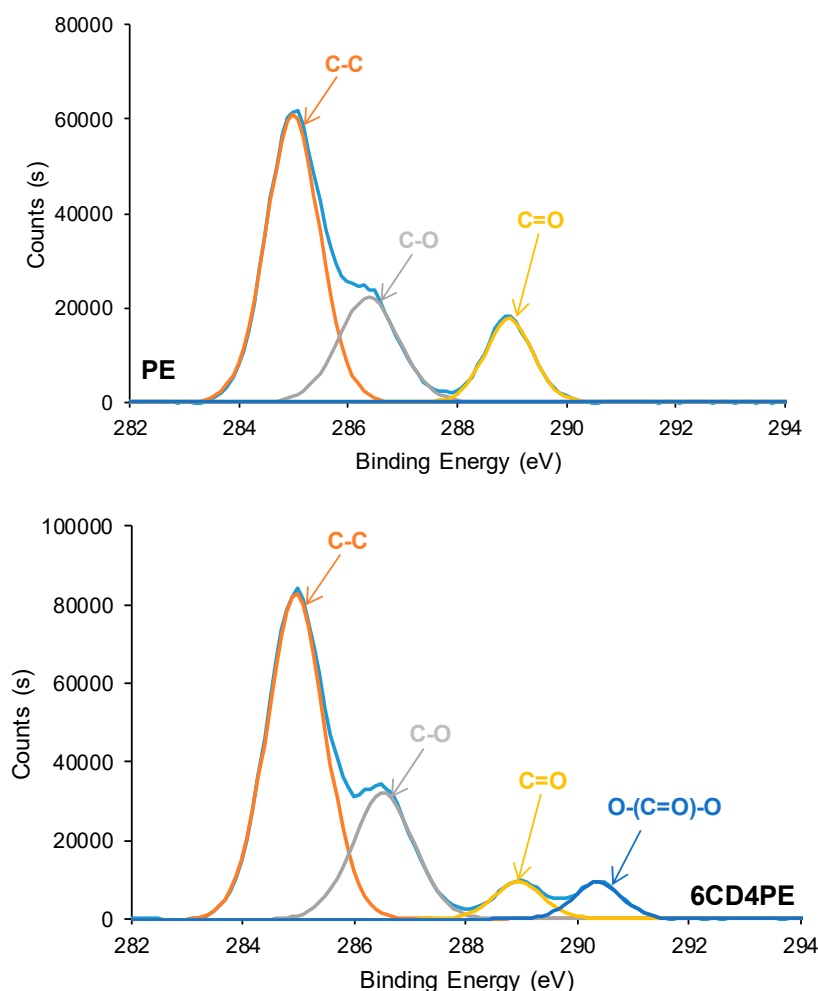


Figure 20. C1s photopeaks of CD, PE and 6CD4PE.

The atomic percentages of the different chemical species on the CD+PE blends surfaces derived from the high resolution C1s photopeaks are shown in Table S5 of the Supplementary Materials file. The variations of the atomic percentages of the C=O and O-(C=O)-O species on CD+PE blends surfaces as a function of their PE content are shown in Figure 21. The atomic percentage of C-O species varies between 27 at.% and 31 at.%, and it is present on both parent polyols. The atomic percentage of C=O species (only present on PE surface) increases from 3 at.% to 7 at.% by increasing the amount of PE from 20 wt.% to 40 wt% and it does not change noticeably by adding more PE. Therefore, the interactions between the PE chains are somewhat similar on the blends surfaces containing 40-80 wt% PE and they are significantly lower than on PE surface. On the other hand, the atomic percentage of O-(C=O)-O species (only present on CD surface) decreases gradually from 10 at.% to 4 at.% by increasing the PE content in the blend, this is an indication of the disruption of the carbonate-carbonate interactions by adding PE.

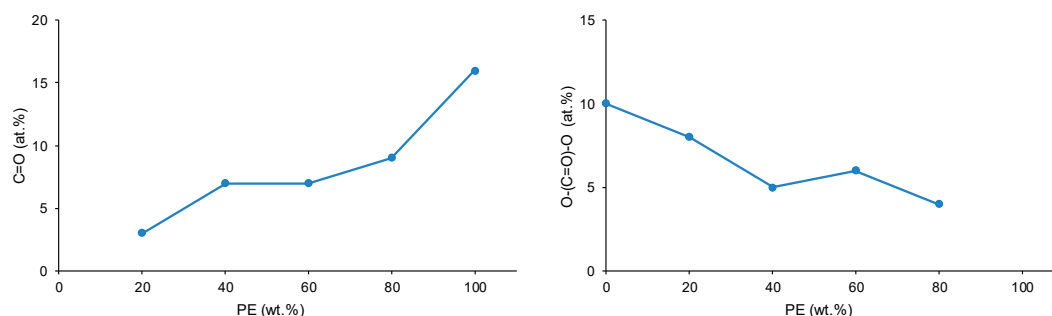


Figure 21. Variation of the C=O (left) and O-(C=O)-O (right) species on CD+PE blends surfaces as a function of PE content. C1s photopeak. XPS experiments.

The surface properties of the polyols and CD+PE blends were also assessed by ethylene glycol contact angles. Figure 22 shows a lower contact angle value on PE than on CD surface, this indicates better wettability. The lower contact angle on PE surface can be ascribed to the existence of a larger number of polar groups than on CD surface (Figures 2 and 3). The contact angle values on the CD+PE blends with PE content lower than 60 wt.% PE decreases continuously, the decrease is more abrupt for the blends containing 40-60 wt.% PE; the contact angle values of the CD+PE blends containing more than 60 wt.% PE are somewhat similar. Therefore, the disruption of the carbonate-carbonate interactions in the blends by adding up to 60 wt% PE is confirmed by ethylene glycol contact angle measurements; the increase of PE content above 60% in the blends does not affect markedly the carbonate-carbonate interactions nor the ester-ester interactions on their surfaces.

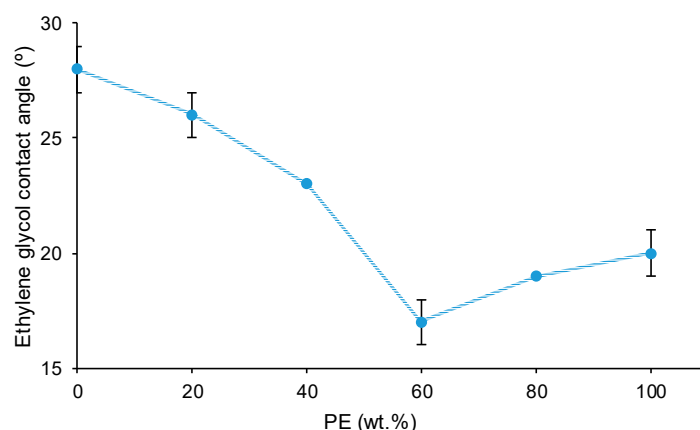


Figure 22. Variation of the ethylene glycol contact angle on polyols and CD+PE blends surfaces as a function of PE content.

The existence of ester-carbonate and carbonate-carbonate interactions may affect the adhesion property of the blends. The self-adhesion properties of the polyols and their blends were assessed by cutting the pieces by half and rejoining them for 30 seconds with the fingers under a mild pressure. After 24h of joint formation, the joined sample were left falling down several consecutive times from a high of 50 cm observing if they de-bond or not. The results of the self-adhesion test of CD is shown in Video S1 of the Supplementary Materials file in which is evidenced that after 7 consecutive fallings, the de-bonding is not produced. The results of the self-adhesion test of PE is shown in Video S2 of the Supplementary Materials file in which is evidenced that after 6 consecutive fallings, the de-bonding is produced. Figure 23 shows the appearance of the CD and PE samples before and after self-adhesion test. The results of the self-adhesion of 2CD8PE is shown, as typical example of the blends, in Video S3 of the Supplementary Materials file in which is evidenced that after 8 consecutive fallings, the de-bonding is not produced. Figure 24 shows the appearance of the CD+PE blends

samples before and after the self-adhesion test, all of them show self-adhesion property likely due to the existence of ester-carbonate and carbonate-carbonate interactions

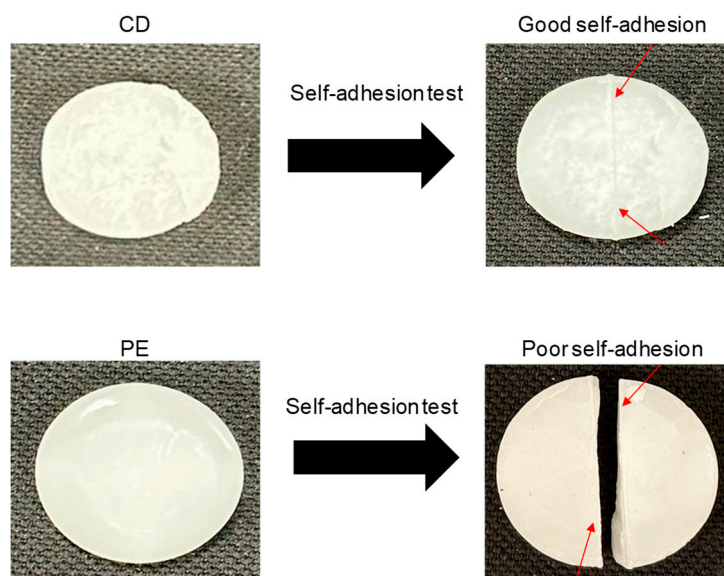


Figure 23. Self-adhesion test of CD and PE test samples.

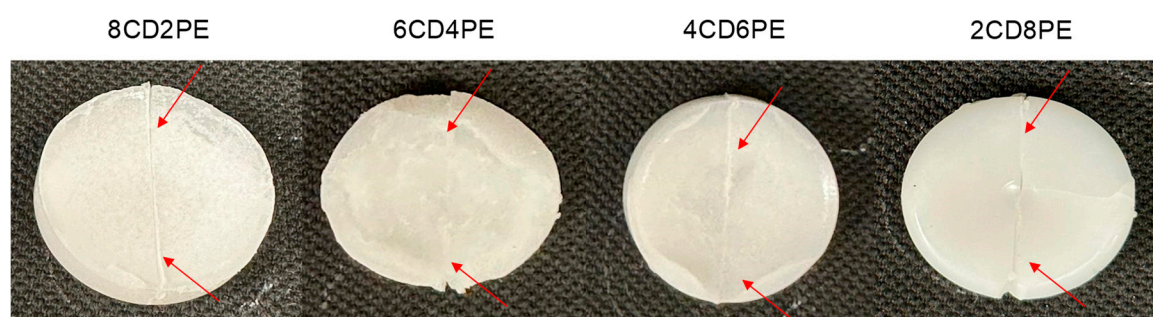


Figure 24. Appearance of the CD+PE test samples after self-adhesion test.

4. Conclusions

The blending of polyols of different nature (PE and CD) and similar molecular weight changed the strength and nature of the interaction between their polar groups, leading to synergic structures in the blends containing less than 50% PE. In other words, the interactions between the polyol chains in the blends differ with respect to the ones in the parent polyols.

The structure of PE showed larger number of structural repeating units and higher number of polar groups than in CD, but the carbonate-carbonate interactions in CD were stronger than the ester-ester interactions in PE. The most ester groups in PE were free and exhibited only one thermal degradation at higher temperature. The curve fitting of the carbonyl region and the lower $I_{C=O}/I_{OC(O)O}$ ratio in the ATR-IR spectrum of CD showed strong interactions between carbonate groups, they led to two thermal degradations at 214 °C (carbonate-carbonate interactions) and 340 °C. Because the higher number of ester groups in PE than carbonate groups in CD, the temperature at which G' decreased in the rheological curves and the temperature at the cross-over of G' and G'' were higher in PE than in CD. Similarly, the ethylene glycol contact angle on PE surface was lower than on CD surface, but PE did not exhibit strong self-adhesion property and CD did, likely due to the stronger carbonate-carbonate interactions.

The blending of CD and PE imparted synergic structural properties, particularly in the ones containing less than 50% PE, they were associated to the disruption of carbonate-carbonate

interactions in CD and the formation of new ester-carbonate and hydroxyl-carbonate interactions. Evidences of the structural changes were provided by IR, DSC, X-ray diffraction, TGA and plate-plate rheology. Thus, the $I_{C=O}/I_{OC(O)O}$ ratios were higher and the C=O stretching band in the ATR-IR spectrum of CD displaced to lower wavenumber in CD+PE blends containing less than 50% PE, and their variation with the amount of PE was not linear. All blends showed five contributions to the carbonyl region (2CD8PE was an exception) and the wavenumber at which each contribution appeared varied depending on the amount of PE. The addition of 20-40% PE to CD caused new contributions due to carbonate-ester, hydroxyl-ester and hydroxyl-carbonate, and the disruption of carbonate-carbonate interactions.

All polyols and blends showed two glass transition temperatures, T_{g1} (due van der Waals interactions between polyols chains) and T_{g2} (due to ester-ester, ester-carbonate and carbonate-carbonate interactions). Due to the formation of ester-carbonate interactions, the highest T_{g1} , T_{g2} , ΔC_{p1} and ΔC_{p2} values corresponded to CD+PE blends with less than 50% PE, and their crystallization temperatures were lower than the one of CD.

The X-ray diffractograms of the CD+PE blends showed a new peak at $2\theta = 24^\circ$ with respect to the parent polyols, this peak was ascribed to the crystallinity associated to ester-carbonate interactions. The addition of only 20% PE disrupted the carbonate-carbonate interactions between CD chains producing new interactions, and the X-ray diffractograms of CD+PE containing less than 50% PE showed somewhat similar features.

The CD+PE blends with less than 50% PE showed three thermal degradations at 220-229 °C, 335-338 °C and 426-436 °C, the thermal degradation at 426-436 °C was associated to ester-carbonate interactions. The thermal degradations at 220-229 °C and 335-338 °C in the blends appeared at higher temperatures than in CD, the higher the PE content, the higher the degradation temperature.

The different structural features in CD+PE blends also affected their viscoelastic properties. The addition of 80 wt.% PE produced the decrease of G' at an intermediate temperature among the ones of PE and CD, due to the disruption of the ester-ester interaction. However, the addition of 20-60 wt.% PE caused less steep decline of G' to lower temperature than in the parent polyols, the higher the CD content, the more noticeable were those changes. All polyols and blends show a cross-over of the storage (G') and the loss (G'') moduli, the temperature at the cross-over in the blend containing 40 wt.% or more PE increased gradually due to the creation of ester-carbonate interactions.

The different interactions between the polyol chains in the CD+PE blends were also evidenced on their surface properties. The atomic percentage of C=O species (only present on PE surface) increased by increasing the amount of PE from 20 wt.% to 40 wt.% and it did not change noticeably by adding more PE. Furthermore, the atomic percentage of O-(C=O)-O species (only present on CD surface) decreased gradually by increasing the PE content in the blend, this indicated the disruption of the carbonate-carbonate interactions by adding PE. On the other hand, the ethylene glycol contact angle values on the blends with PE content lower than 60 wt.% PE decreased continuously, this agreed with the disruption of the carbonate-carbonate interactions in the blends.

Finally, all CD+PE blends showed self-adhesion property which seemed related to the existence of ester-carbonate and carbonate-carbonate interactions.

Supplementary Materials: The following supporting information can be downloaded at the website of this paper posted on Preprints.org, Figure S1: Curve fitting of the carbonyl stretching region of the ATR-IR spectrum of 4CD6PE; Figure S2: Variation of the storage (G') and loss (G'') moduli of CD as a function of the temperature; Figure S3: C1s photopeaks of different CD+ PE blends; Table S1: Assignment of the main absorption bands in the ATR-IR spectrum of CD; Table S2: Assignment of the main absorption bands in the ATR-IR spectrum of PE; Table S3: Assignment of the main absorption bands in the ATR-IR spectra of CD+PE blends; Table S4: Wavenumbers of species in the carbonyl stretching region of the ATR-IR spectra of the polyols and CD+PE blends; Table S5: Chemical species on the polyols and CD+PE blend surfaces. C1s photopeak. XPS experiments; Video S1: Self-adhesion test of CD; Video S2: Self-adhesion test of PE; Video S3: Self-adhesion test of 2CD8PE.

Author Contributions: Conceptualization, J.M.M.-M.; methodology, J.M.M.-M.; formal analysis, Y.P.-A. and J.M.M.-M.; investigation, Y.P.-A.; resources, J.M.M.-M.; data curation, Y.P.-A.; writing—original draft preparation, Y.P.-A.; writing—review and editing, J.M.M.-M.; supervision, J.M.M.-M.; project administration,

J.M.M.-M.; funding acquisition, J.M.M.-M. All authors have read and agreed to the published version of the manuscript.

Funding: This research received no external funding.

Institutional Review Board Statement: Not applicable.

Data Availability Statement: Not applicable.

Acknowledgments: The authors thank Synthesia (Barcelona, Spain) and UBE Chemical Europe (Castellón, Spain) for supplying the polyols used in this study.

Conflicts of Interest: The authors declare no conflict of interest.

References

1. Saunders J. H. Raw Materials. In *Polyurethanes: Chemistry and Technology*; Interscience: New York, USA, 1962; pp. 17–61. ISBN 0-88275-740-7.
2. Jofre-Reche, J. A.; García-Pacios, V.; Costa, V.; Colera, M.; Martín-Martínez, J. M. Role of the interactions between carbonate groups on the phase separation and properties of waterborne polyurethane dispersions prepared with copolymers of polycarbonate diol. *Prog. Org. Coat.* **2015**, *88*, 199–211, DOI: 10.1016/j.porgcoat.2015.06.029.
3. Chen, T. K.; Chui, J. Y.; Shieh, T. S. Glass transition behaviors of a polyurethane hard segment based on 4, 4'-diisocyanatediphenylmethane and 1, 4-butanediol and the calculation of microdomain composition. *Macromolecules* **1997**, *30*, 5068–5074, DOI: 10.1021/ma9618639.
4. Velankar, S.; Cooper, S. L. Microphase separation and rheological properties of polyurethane melts. 1. Effect of block length. *Macromolecules* **1998**, *31*, 9181–9192, DOI: 10.1021/ma9811472.
5. Saiani, A.; Daunch, W. A.; Verbeke, H.; Leenslag, J. W.; Higgins, J. S. Origin of multiple melting endotherms in a high hard block content polyurethane. 1. Thermodynamic investigation. *Macromolecules* **2001**, *34*, 9059–9068, DOI: 10.1021/ma0105993.
6. Saiani, A.; Rochas, C.; Eeckhaut, G.; Daunch, W. A.; Leenslag, J. W.; Higgins, J. S. Origin of multiple melting endotherms in a high hard block content polyurethane. 2. Structural investigation. *Macromolecules* **2004**, *37*, 1411–1421, DOI: 10.1021/ma034604+.
7. Saiani, A.; Novak, A.; Rodier, L.; Eeckhaut, G.; Leenslag, J. W.; Higgins, J. S. Origin of multiple melting endotherms in a high hard block content polyurethane: Effect of annealing temperature. *Macromolecules* **2007**, *40*, 7252–7262, DOI: 10.1021/ma070332p.
8. Niemczyk, A.; Piegat, A.; Olalla, Á. S.; El Fray, M. New approach to evaluate microphase separation in segmented polyurethanes containing carbonate macrodiol. *Eur. Polym. J.* **2017**, *93*, 182–191, DOI: 10.1016/j.eurpolymj.2017.05.046.
9. Onder, K.; Peters, R. H.; Spark, L. C. Melting and transition phenomena in some polyester-urethanes. *Polymer* **1972**, *13*, 133–139, DOI: 10.1016/S0032-3861(72)80008-9.
10. Desai, S.; Thakore, I. M.; Sarawade, B. D.; Devi, S. Effect of polyols and diisocyanates on thermo-mechanical and morphological properties of polyurethanes. *Eur. Polym. J.* **2000**, *36*, 711–725, DOI: 10.1016/S0014-3057(99)00114-7.
11. Oertel, G.; Abele, L. Raw Materials. In *Polyurethane handbook: chemistry, raw materials, processing, application, properties*; Ed. Günter Oertel with contributions from L. Abele; Hanser: Munich, Germany, 1985; pp. 42–62. ISBN 3-446-1371-1.
12. Hepburn, C. Chemistry and basic intermediates. In *Polyurethane elastomers*, 2nd ed.; Elsevier Science: London, England, 1991; pp. 1–28. ISBN 1-85166-589-7.
13. Fuensanta, M.; Jofre-Reche, J. A.; Rodríguez-Llansola, F.; Costa, V.; Iglesias, J. I.; Martín-Martínez, J. M. Structural characterization of polyurethane ureas and waterborne polyurethane urea dispersions made with blends of polyester polyol and polycarbonate diol. *Prog. Org. Coat.* **2017**, *112*, 141–152, DOI: 10.1016/j.porgcoat.2017.07.009.
14. Chemical & polymers blog. Available online: <https://www.gantrade.com/blog/ultimate-performance-polyurethanes-based-on-polycarbonate-diols> (accessed on 8 October 2023).
15. Foy, E.; Farrell, J. B.; Higginbotham, C. L. Synthesis of linear aliphatic polycarbonate macroglycols using dimethylcarbonate. *J. Appl. Polym. Sci.* **2009**, *111*, 217–227, DOI: 10.1002/app.28887.
16. Bicerano & associates consulting. Available online: <https://polymerexpert.biz/blog/144-polycarbonate-polyols> (accessed on 11 November 2018).
17. García-Pacios, V.; Costa, V.; Colera, M.; Martín-Martínez, J. M. Affect of polydispersity on the properties of waterborne polyurethane dispersions based on polycarbonate polyol. *Int. J. Adhes. Adhes.* **2010**, *30*, 456–465, DOI: 10.1016/j.ijadhadh.2010.03.006.

18. García-Pacios, V.; Costa, V.; Colera, M.; Martín-Martínez, J. M. Waterborne polyurethane dispersions obtained with polycarbonate of hexanediol intended for use as coatings. *Prog. Org. Coat.* **2011**, *71*, 136-146, DOI: 10.1016/j.porgcoat.2011.01.006.
19. Kojio, K.; Furukawa, M.; Nonaka, Y.; Nakamura, S. Control of mechanical properties of thermoplastic polyurethane elastomers by restriction of crystallization of soft segment. *Materials* **2010**, *3*, 5097-5110, DOI: 10.3390/ma3125097.
20. Haab, Y. M.; Kim, Y. O.; Ahn, S.; Lee, S. K.; Lee, J. S.; Park, M.; Chung, J. W.; Jung, Y. C. Robust and stretchable self-healing polyurethane based on polycarbonate diol with different soft-segment molecular weight for flexible devices. *Eur. Polym. J.* **2019**, *118*, 36-44, DOI: 10.1016/j.eurpolymj.2019.05.031.
21. García-Pacios, V.; Colera, M.; Iwata, Y.; Martín-Martínez, J. M. Incidence of the polyol nature in waterborne polyurethane dispersions on their performance as coatings on stainless steel. *Prog. Org. Coat.* **2013**, *76*, 1726-1729, DOI: 10.1016/j.porgcoat.2013.05.007.
22. Gündüz, G.; Kisakürek, R.R. Structure-property study of waterborne polyurethane coatings with different hydrophilic contents and polyols. *J. Dispersion Sci. Technol.* **2004**, *25*, 217-228, DOI: 10.1081/DIS-120030668.
23. Kwak, Y. S.; Park, S. W.; Lee, Y. H.; Kim, H. D. Preparation and properties of waterborne polyurethanes for water vapor permeable coating materials. *J. Appl. Polym. Sci.* **2003**, *89*, 123-129, DOI: 10.1002/app.12128.
24. Meng, Q. B.; Lee, S. I.; Nah, C.; Lee, Y. S. Preparation of waterborne polyurethanes using an amphiphilic diol for breathable waterproof textile coatings. *Prog. Org. Coat.* **2009**, *66*, 382-386, DOI: 10.1016/j.porgcoat.2009.08.016.
25. Cakić, S. M.; Ristić, I. S.; Krakovský, I.; Stojiljković, D. T.; Bělský, P.; Kollová, L. Crystallization and thermal properties in waterborne polyurethane elastomers: Influence of mixed soft segment block. *Mater. Chem. Phys.* **2014**, *144*, 31-40, DOI: 10.1016/j.matchemphys.2013.12.008.
26. Cakić, S. M.; Ristić, I. S.; Marinović-Cincović, M.; Špírková, M. The effects of the structure and molecular weight of the macrodiol on the properties polyurethane anionic adhesives. *Int. J. Adhes. Adhes.* **2013**, *41*, 132-139, DOI: 10.1016/j.ijadhadh.2012.11.001.
27. Kardar, P. Preparation of polyurethane microcapsules with different polyols component for encapsulation of isophorone diisocyanate healing agent. *Prog. Org. Coat.* **2015**, *89*, 271-276, DOI: 10.1016/j.porgcoat.2015.09.009.
28. Rahman, M. M.; Suleiman, R.; Zahir, M. H.; Helal, A.; Kumar, A. M.; Haq, M. B. Multi Self-healable UV shielding polyurethane/CeO₂ protective coating: the effect of low-molecular-weight polyols. *Polymers* **2020**, *12*, 1947, DOI: 10.3390/polym12091947.
29. Žagar, E.; Grdadolnik, J. An infrared spectroscopic study of H-bond network in hyperbranched polyester polyol. *J. Mol. Struct.* **2003**, *658*, 143-152, DOI: 10.1016/S0022-2860(03)00286-2.
30. Mishra, A. K.; Chattopadhyay, D. K.; Sreedhar, B.; Raju, K. V. S. N. FT-IR and XPS studies of polyurethane-urea-imide coatings. *Prog. Org. Coat.* **2006**, *55*, 231-243, DOI: 10.1016/j.porgcoat.2005.11.007.

Disclaimer/Publisher's Note: The statements, opinions and data contained in all publications are solely those of the individual author(s) and contributor(s) and not of MDPI and/or the editor(s). MDPI and/or the editor(s) disclaim responsibility for any injury to people or property resulting from any ideas, methods, instructions or products referred to in the content.